2

# Fracture Toughness Determinations by Means of Indentation Fracture

Enrique Rocha-Rangel
*Universidad Politécnica de Victoria*
*México*

## 1. Introduction

The assessment of fracture toughness ($K_{IC}$) on fragile materials such as ceramics or composites through conventional methods can be arduous. Recently, an alternative route referred to as the Indentation Fracture technique has been widely accepted with this purpose and extensively reported in literature (Weisbrod & Rittel, 2000; Plaza, 2003; Evans & Charles, 1976; Niihara et al., 1982). Different authors have derived math equations series as to fine tune and match with $K_{IC}$ determination; those equations are based in the lineal mechanical fracture theory (Wang, 1996). The indentation fracture method and its application procedure are described in this chapter, whereas typical problems involved in the test are shown. $Al_2O_3$-based composites with different reinforced metals fabricated by both; liquid and solid pressureless sintering of an intensive mechanical mixture of powders were used as studied materials.

Ceramic materials have properties of great interest for various structural applications, specifically those that take advantage of their high hardness, chemical and thermal stability in addition to their high stiffness. However, their great fragility has severely limited their applications, although they have developed ceramic with reinforcement materials precisely to increase the toughness of the same (Miranda et al., 2006; Konopka & Szafran, 2006; Marci & Katarzyna, 2007; Travirskya et al., 2003; Sglavo, 1997). One of the macroscopic properties that characterize the fragility of a ceramic is the fracture toughness ($K_{IC}$). The fracture toughness describes the ease with which propagates a crack or defect in a material. This property can be assessed through various methods such as: Analytical solution, solution by numerical methods (finite element, boundary integral, etc.). Experimental methods such as: complianza, fotoelasticity, strain gauge, etc. and indirect methods such as: propagation of fatigue cracks, indentation, fractography, etc. The choice of method for determining the fracture toughness depends on the availability of time, resources and level of precision required for the application. In practice, measurements of $K_{IC}$ require certain microstructural conditions on the material to allow propagation of cracks through it in a consistent manner. The strength of materials is governed by the known theory of Griffith, which relates the strength (S) with the size of the defect or crack (c) by $S = YK_{IC}/c^{1/2}$. This expression suggests the need to reduce the grain size and processing defects in the final microstructure to optimize the mechanical performance. Moreover, with increasing $K_{IC}$, resistance becomes less dependent on the size of the defect, thereby producing a more tolerant material to cracking. Due to high elastic modulus and low values of $K_{IC}$ in brittle materials, achieving in them a stable crack growth is complicated and sometimes it is necessary sophisticated

measurement equipments and complex sample geometries (Wessel, 2004). The problem with applying these methods to evaluate $K_{IC}$ is that required laborious procedures and only get one result by sample, being necessary multiple measurements to obtain reliable statistical results. In this sense many simple methods have been proposed to avoid these difficulties. One particularly attractive procedure due to its simplicity for routine evaluations of engineering materials is the indentation fracture (IF) method.

Although the IF method can only measure approaches of the values of $K_{IC}$, is a convenient technique for evaluation of many brittle engineering materials. This technique is based on normalized standards hardness tests (ASTM E1820 - 09e1 Standard Test Method for Measurement of Fracture Toughness, 2008 and ASTM C 1327-99, Standard Test Method for Fracture Toughness at Room Temperature of Advanced Ceramics, 1999. Assuming the presence of a preexisting, sharp, fatigue crack, the material fracture toughness values identified by this test method characterize its resistance to: (1) fracture of a stationary crack, (2) fracture after some stable tearing, (3) stable tearing onset, and (4) sustained stable tearing. This test method is particularly useful when the material response cannot be anticipated before the test, making reliable they obtained result.

These fracture toughness values may serve as a basis for structural flaw tolerance assessment. Awareness of differences that may exist between laboratory test and field conditions is required to make proper flaw tolerance assessment.

The test is relatively simple to implement and requires only a standard micro hardness tester. A small piece of material with a stress free surface and cracks is enough as test sample. The method, however, is not suitable for materials with values of $K_{IC}$, below 1 MPa $\cdot m^{1/2}$, significant ductility, large grain size and heterogeneous microstructures.

## 2. Antecedents

By the mid-60 began to apply empirically the concept of fracture mechanics to ceramic. The development of science has run parallel to the indentation techniques which helped to determine the resistance to penetration of the indenter in ceramics systematically. However, the most important development was the discovery of the transformation of the zirconia and the consequent increase in fracture toughness. From there they spent the previous design of the material and systematic study on the basis of the manufacture, characterization, testing and modeling. Another, important advance was the discovery that the addition of second phase substances such as fibers and spheroids particles improved mechanical properties such as fracture toughness (Konopka & Szafran, 2006; Travirskya et al., 2003; Bosch, 1990; Lieberthal & Kaplan; 2001). Finally, it started working with cermets, it means ceramic composites with second phase dispersed particles produced by particles processing or made directly by oxidation of metal.

However, progress in understanding the mechanisms of increasing fracture toughness has been slow for various reasons as the difference between the methods of measuring it, which raises questions about its usefulness. On the other hand, the most reliable methods of measurement tests require large numbers of samples which is not easy and possible in all ceramics.

### 2.1 Fracture definition

The fracture is the separation of a material under stress action. The fracture occurs by crack initiation and propagation (Figure 1). In this case the fault occurs with a small plastic deformation. The most important atomic mechanism is the breaking of atomic bonds due to

the application of static loads. Although, theoretically the fracture can be caused by shearing forces, the majority of cases correspond to the application of normal, tension or bending stress.

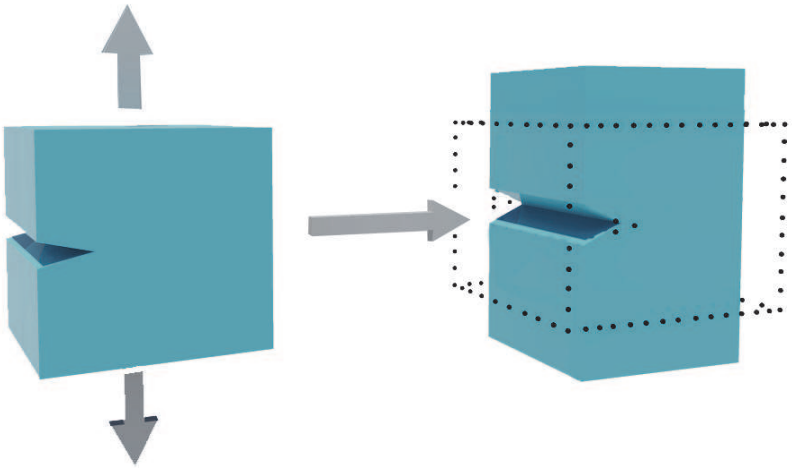

Fig. 1. Open crack and deformation of a body that is under tensile forces.

The normal stress is the most effective in breaking atomic bonds. The fracture can be ductile or brittle and involves a small or large consumption of energy, respectively (Figure 2). The comparison between both types of fracture shows always a sudden collapse in brittle fracture due to low energy absorption, originating from external stresses.

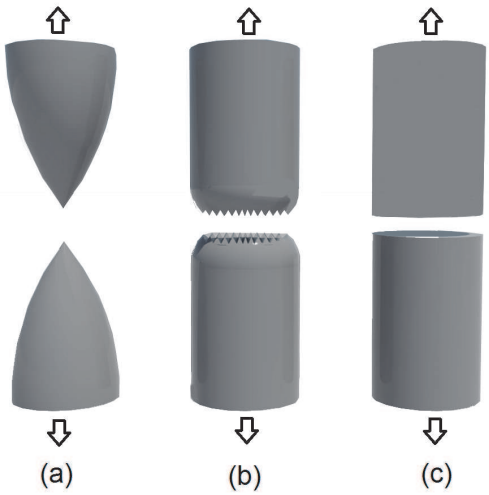


Fig. 2. Brittle vs. Ductile fracture (a) Very ductile, soft metals (e.g. Pb, Au) at room temperature, other metals, polymers, glasses at high temperature. (b) Moderately ductile fracture, typical metals (c) Brittle fracture, cold metals and ceramics.

### 2.2 Fracture and energy balance

It is generally conventionally considered that Griffith (1920) with his work: "The phenomena of rupture and flow in solids" was the first who introduced a scientific approach on the fracture in solids. The theory of linear elastic fracture mechanics began to be developed at that time. The Griffith fracture mechanics allowed to obtain a powerful criterion to predict crack propagation demonstrating to be generalizable to many types of materials and still remain valid.

Consider an infinite plate of unit thickness with a crack of length 2c is subjected to a tensile stress as shown in Figure 3.

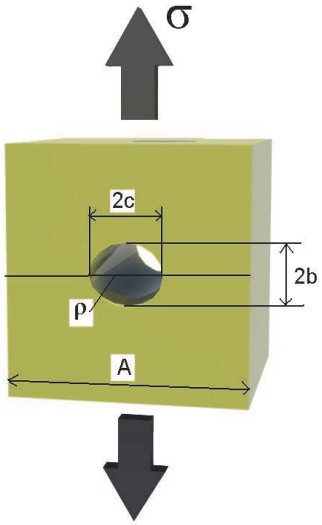


Fig. 3. Infinite plate of unit thickness with a crack of length 2c under tensile stress.

Griffith observed experimentally that small imperfections had a destructive influence on the materials much more than large and involved that in an energy balance not only care about the potential energy of external forces (W) and the stored elastic energy (UO), but another had not previously considered: the surface energy (US).

The surface energy (US) is needed to create new surfaces, incorporating work. For example, the blow and grow the surface of a soap bubble is required to make a job.

Correlated energies displayed are:

U - Total system energy

UO - Energy elastic plate with no cracks with applied forces (constant)

EU - elastic energy introduced to take place the opening of the crack

W - Work of external forces on the body

US - Energy associated with the "resistance" that opposes the material to the creation of new surfaces

Where:

$$U = U_0 + U_E - W + U_s \tag{1}$$

The parameters W and EU are associated with each other because they both promote the formation and propagation of the crack, while US represents the "resistance" that the material opposes to the creation of new surfaces, such as those generated by cracks.
Inglis proposed a solution that Griffith retums by the assumption that there is an atomic break caused by the crack, which is expected in brittle materials, such as ceramic. In a harmonic oscillator model ($a_o$ is the atomic separation), once the springs have collapsed due to high normal stress the crack propagates in a perpendicular plane as shown in Figure 4.

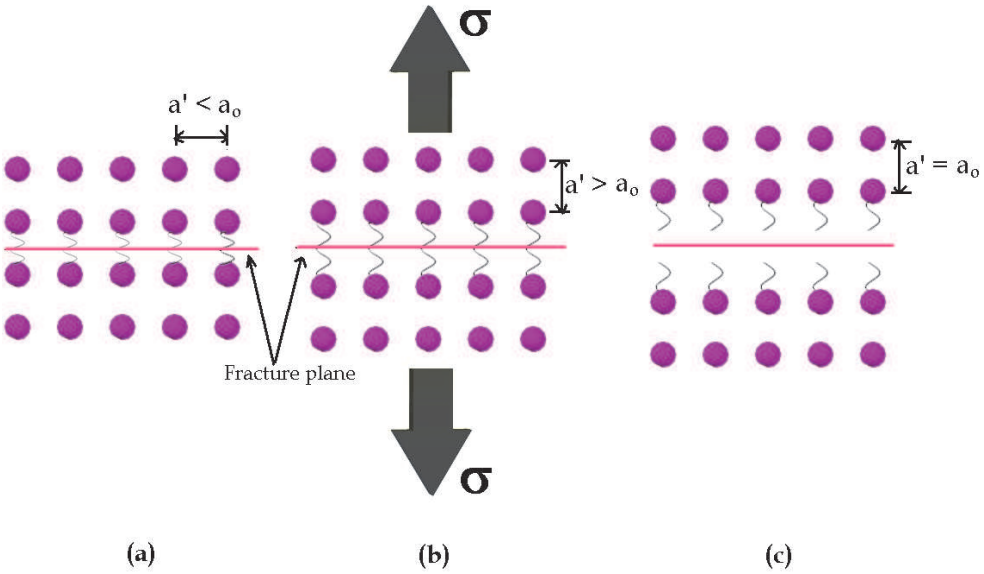


Fig. 4. Atomic break caused by the crack. $a_o$ is the atomic separation, once the springs have collapsed due to high normal stress the crack propagates in a perpendicular plane.

Griffith's equation states:

$$U_e - W = -\frac{\pi\sigma^2 c^2}{E} \tag{2}$$

If it is consider this "elastic capacity" of material per unit area (dA) of the cracks generated, it can be defined a magnitude G.

$$G = \frac{d(U_E - W)}{dA} = \frac{d(U_E - W)}{2dc} \tag{3}$$

Where it is suppose a unitary depth of the crack and a length dc. The number 2 is because there are two surfaces created by crack.
The term "G" means the energy supplied per unit area as the elastic capacity of the body to create new surfaces (those of the cracks). It requires a continuous supply of stored elastic energy in the body to continue the propagation of a crack once initiated. From body parts with smaller loads comes the energy supply, although the main contribution is from the

stress concentration areas that cause local increase of the stress. Until several years ago, G was the parameter used to measure the "toughness" and then was replaced by K, the "intensity of stress". G may be considered (dimensionally) as a force (supplied by the body) per unit length of the crack, or force of crack propagation. Applying the equations (2) and (3) we have:

$$G = -\frac{\pi\sigma^2 c}{E} \tag{4}$$

Where:
σ - Tensile or bending stress of the material.
c - Semiaxis of the crack (assumed elliptical) in the direction perpendicular to the stress
E – Elasticity modulus
Inglis assumed that the difference between the elastic energy stored in the body and dissipated by the crack plus the external work exerted on the body by the applied normal stress is proportional to the elastic energy contained in a circle of radius c (2a) as can be seen in Figure 5.

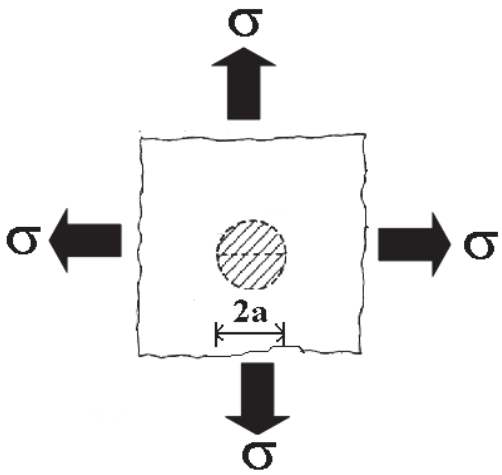


Fig. 5. Applied normal stress is proportional to the elastic energy contained in a circle of radius c (2a).

### 2.3 Cracking modes and the concept of fracture toughness ($K_{IC}$)

The stress-intensity Factor (K) is a quantitative parameter of fracture toughness determining a maximum value of stress which may be applied to a specimen containing a crack of a certain length.
Depending on the direction of the specimen loading and the specimen thickness, three types of stress-intensity factors are used: $K_{IC}$ $K_{IIC}$ $K_{IIIC}$.
All the stress fields near cracks can be deduced from the three load shapes that cause the formation of three types of cracks, called "ways of cracking". As shown in Figure 6, the mode I is the crack opening by traction. The II is sliding on a plane and the third involves a lateral movement or "tearing" of the material.

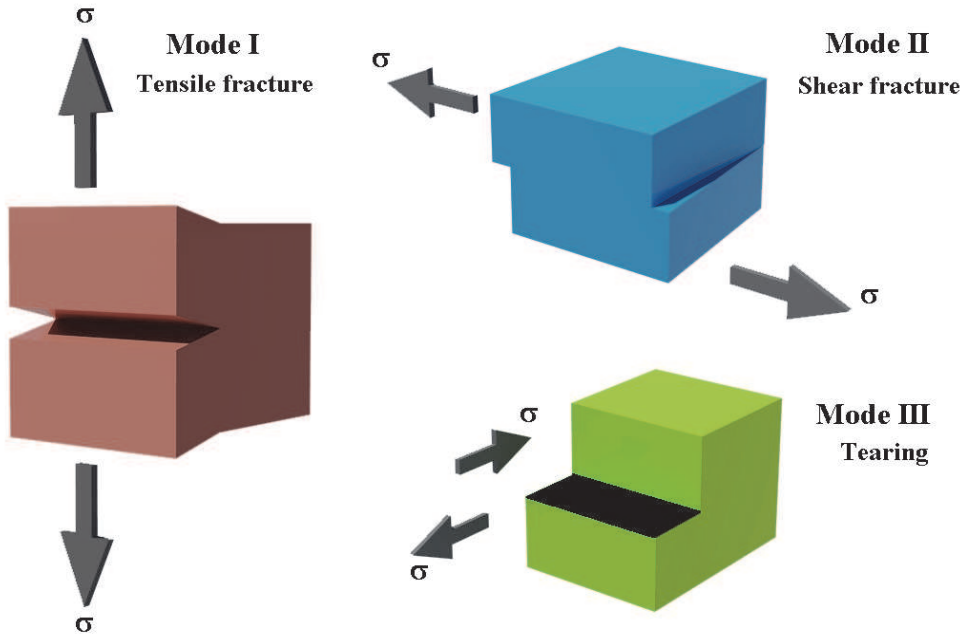


Fig. 6. Fracture modes.

The fracture toughness ($K_{IC}$) is a "threshold property" so that (theoretically) above or below face value there is or not crack propagation, respectively. Thus, from the standpoint of stress, this is the "stimulus" and the crack is the response to stimulation. The fracture toughness (or, ductility) enables an adequate redistribution of effort, as it is expected that local efforts have higher than average, and if local plastic flow would be possible for another part of the structure without stress bear so great, absorb the load. Hence, the importance in materials technology for finds procedures to increase $K_{IC}$. The fracture toughness depends on the elastic energy dissipated (Wang, 1996). Therefore, if the material has a high ability to dissipate elastic energy during crack propagation, without a catastrophic failure, we can say that the material has high fracture toughness.

Since the critical value of K is $K_{IC}$ in the crack propagation mode I, one can expect a parabolic proportionality of K in relation to E, so that K increases with E, giving the equation 5. In fact in ceramics there is an erratic behavior and in some cases there was no simultaneous increase in $K_{IC}$ and E. This may be due to the presence of other mechanisms such as microplasticity and the second phase substances (Wessel, 2004).

$$K_{IC} = \sqrt{2\gamma_s E} \tag{5}$$

The crack propagation occurs when G (ec.4) reaches a critical value Gc, which is equal to $dU_S/dA$ that contains the term dissipation of energy by the formation of new surfaces in a material and is the "resistance" or opposition to it. Also known as R. Therefore, the crack propagation occurs when G becomes R, is to mean when is achieved and exceed a critical value. Obtaining a metastable equilibrium.

$$G_c = R \tag{6}$$

Assuming that $\sigma_c$ and $C_c$ are the stress and the half of crack length at the critical point respectively, we obtain:

$$R = \frac{\pi\sigma_c^2 c_c^2}{E} \tag{7}$$

In this case the crack propagates, but the increase in length is unstable and the total energy U [equation (1)] decreases. In contrast, if a stress is applied $\sigma 1 < \sigma$ cr then

$$G = \frac{\pi\sigma_1^2 c_{cr}}{E} \tag{8}$$

The crack does not propagate because

$$\frac{dU}{dc} < 0 \tag{9}$$

### 2.4 Use of hardness to characterize toughness and fragility (Correlations)

A systematic exposition of the expose above, allows to realize a conceptual connection with the measurement of another properties from hardness (H). It is possible to correlate the measurement of the hardness of the ceramic samples with different microstructural characteristics and properties such as fracture toughness, the extent of the crack and the elastic modulus. A possible sequence

1. The stress field is formed from:
   a. The applied load
   b. The stress field in the volume of the sample around the indented area that responds to conditions of elasticity (dependent of Young's modulus, E) or plastic flow of material (microplasticity) around the indented area. Since there are stresses when the load is removed, they are called residuals.
2. The maximum stress due to the application of the load in the volume under the area of indentation occurs at the interface between the elastic and plastic zone, which in turn creates microcracks that depend on the population of imperfections surface and nucleation mechanisms of the sliding planes of the material.
3. On the surface the indenter causes compression and not tension and acts not opposing to residual stresses.
4. When is retired the indenter the compression on the surface decreases to zero.
5. Residual stresses (which have no opposition and are of the order Hv/20) acting against the surface and cause radial cracks on the surface, visible under the microscope on slick surfaces. These are radial cracks.
6. The radial and meridional cracks combine to form semi-elliptical crack surface and their diameter is about twice the depth of the crack.
7. Radial cracks fully developed are in mechanical equilibrium and their dimensions are determined from the $K_{IC}$. Thus this let to measure the $K_{IC}$.

Lawn and other researchers (Marshall & Lawn, 1986) formulated the view that residual stresses do not contribute to a specific factor to the fracture toughness but instead affect the length 2c of the cracks (see Figure 7). The basic equations that determine this parameter and hardness are:

$$H_V = \frac{P}{\alpha a^2} \tag{10}$$

$$K_c = \frac{P}{\beta c^{2E}} \tag{11}$$

Where:
α, β - constants
a - half length of the indentation diagonal
c - half length of the crack generated by indentation
E – elasticity modulus
P - applied load in the sample for hardness testing
$K_C$ - Fracture Toughness

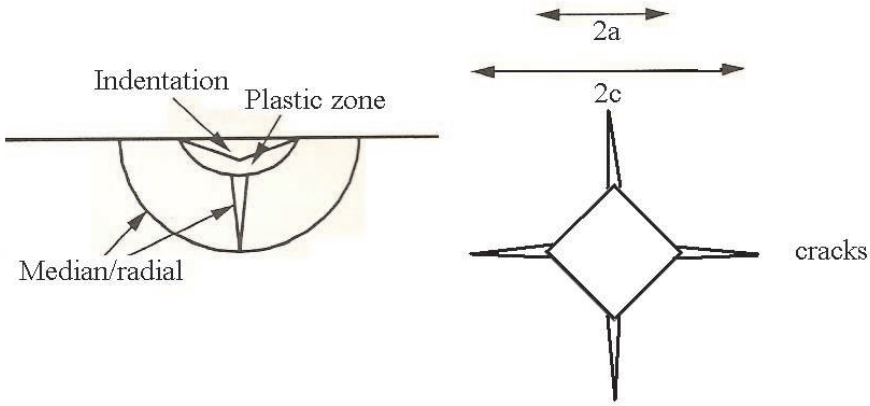


Fig. 7. Cracking around hardness indentation.

α depends on the geometry of the indenter and in the case of those are Vickers type its value is 2. On the other hand β is a constant but with more complex geometry that considers the effects of interaction between the free surface of the specimen and the cracks generated configurations. Its value is obtained experimentally.
When c >> a, the cracks centers can be considered at the point of the footprint of the apex of the indenter and the $K_r$ contribution of residual stress to $K_C$ is expressed as:

$$K_\gamma = \frac{\beta_\Gamma P}{C^{Z,2}} \tag{12}$$

In this equation βr is a constant proportional to $\sqrt{\frac{E}{H_V}}$. Since the ceramic with weak bonds such as: ionic or ionic-covalent, have lower values of E compared to those with covalent bonds, present also less hardness and less residual stresses too. The fracture toughness is also lower, as seen in all equations use "general" to be presented below.

When mechanical equilibrium is reached and no further propagation of cracks during the loading or after it was removed then:

$$K_{\gamma} = K_C = \frac{\beta_T P}{C^{1E}} = a_r \sqrt{\frac{E}{H_{\lambda}}} \frac{P}{C^{1E}} \tag{13}$$

Applying equation (10):

$$K_C = a_r \sqrt{\frac{E}{H_{\lambda}}} \frac{H_{\gamma} a a^2}{C^{1E}} = 0.032 \sqrt{\frac{E}{H\gamma}} \frac{H\gamma a^2}{C^{1E}} \tag{14}$$

Where $\alpha_r = 0.016 \pm 0.004$ y $\alpha = 2$ as was specified earlier.
All formulas are referring to this result, although some minor changes were made in the coefficient or in the exponent to adjust the results to the experimental values. The original formula is of Lawn.

$$K_C = 0,028 \sqrt{\frac{E}{H_V}} H V a^{\frac{1}{2}} \left(\frac{c}{a}\right)^{-1,5} \quad \text{(Lawn)} \tag{15}$$

Another well-known formula is the (Evans and Charles, 1976).

$$K_{IC} = 0.16\ (c/a)^{-1.5}\ (Ha^{1/2}) \quad \text{(Evans y Charles)} \tag{16}$$

(Niihara, 1982) established that:

$$K_C = 0,067 \left(\frac{E}{H_V}\right)^{0,4} H_V \alpha^{0,5} \left(\frac{c}{a}\right)^{-1,5} \quad \text{(Niiihara)} \tag{17}$$

(Antis et al., 1981) did not replace the value of P as a function of HV and found this equation that is virtually the same of Lawn:

$$K_c = 0,016 \left(\frac{E}{H_V}\right)^{0,5} \frac{P}{c^{1,5}} \quad \text{(Antis)} \tag{18}$$

A final equation is that of Bhat, 2006)

$$K_{IC} = 1,59x10^5 E^{0,4} P^{0,6} a^{-0,7} \left(\frac{c}{a}\right)^{-0,36} \quad \text{(Bhat)} \tag{19}$$

In the equation of Bhat elasticity modulus E is expressed in Pa, the load P in grams and both a and c in microns. The result is given in MPa $\cdot m^{0.5}$ and it is assumed $c/a > 3$.

## 3. The indentation fracture (IF) method

As has be mentioned earlier the indentation fracture method, is derived from the experimental procedure commonly followed in hardness tests, it consists in relate the lengths of the cracks shown in Figure 8, growing in the corners of the Vickers indentation when a load (P) is applied, with the toughness of the material.

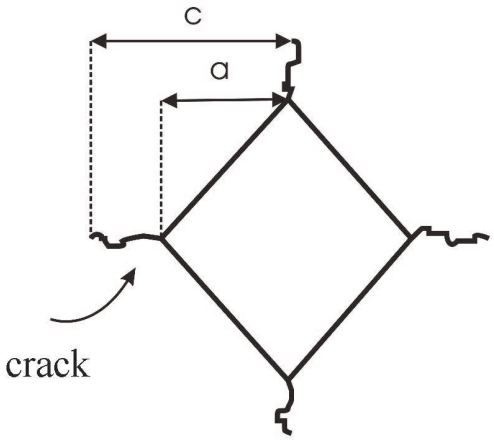


Fig. 8. Vickers indentation mark.

To calculate $K_{IC}$ by this method they have developed a number of equations, some of which require the values of Young and Poisson modulus for their use in addition to the hardness test results. The equations are divided into two groups: empirical and experimental. One of the most used among the empirical group is the equation (16) proposed by Evans. While equation (17) proposed by Niihara is one of the most experimental frequently used

$$K_{IC} = 0.16\,(c/a)^{-1.5}\,(Ha^{1/2}) \qquad \text{(Evans y Charles) (16)}$$

$$K_C = 0,067\left(\frac{E}{H_V}\right)^{0,4} H_V \alpha^{0,5}\left(\frac{c}{a}\right)^{-1,5} \qquad \text{(Niihara) (17)}$$

Also:

$$H = 1.8P/a^2 \qquad (20)$$

Where:
$K_{IC}$ = Fracture toughness (MPa·$m^{1/2}$)
H = Vickers hardness (MPa)
E = Young modulus (MPa)
P = Test load in Vickers hardener (MPa)
c = Average length of the cracks obtained in the tips of the Vickers marks (microns)
a = Half average length of the diagonal of the Vickers marks (microns)

### 3.1 Applications of the IF method

With the idea to observe the application of the IF method investigations about the production of $Al_2O_3$-based composites with different reinforcement metals and intermetallics have been carried out. The synthesis of composites materials has been made by means of both; liquid and solid pressureless sintering of an intensive mechanical mixture of powders.

### 3.2 Experimental procedure

The starting raw material were powders of $Al_2O_3$, FeO, NiO, $TiO_2$ and $ZrO_2$ (99.9 %, 1 μm, Sigma, USA) and powders of aluminum, cobalt, copper, iron, molybdenum, nickel, titanium and zirconium (99.9 % purity, 1-2 μm, Aldrich, USA). For the composites reinforced with pure metals the amount of powders used was one that allowed obtaining $Al_2O_3$-based composites with 10 vol. % of the respective metal. For the composites reinforced with intermetallics, they were used as oxides of the respective metal for the in situ synthesis of the corresponding intermetallic phase. The sum of the starting materials; was fitted to the necessary amounts to form the products indicated in reaction (21) with 10 vol. % of each intermetallic phase.

$$Me_xO_y + Al \rightarrow Me_xAl_y + Al_2O_3 \quad (21)$$

Where: Me can be any of the next metals; Fe, Ni, Ti or Zr.

The processing and characterization of the composites were as follows: The weighted powders were put under a process of dry mix-milling at a speed of rotation of 300 rpm for 12 h, with the help of a horizontal mill (Cole Parmer, Labmill) using as milling elements balls of stabilized $ZrO_2$ (YSZ), the weight ratio of balls/powders was of 25:1. The powder mixtures were then fabricated into ten cylindrical samples of each composition with dimensions of 20 mm in diameter and 3 mm in thickness; this was done by uniaxial pressing of up to 200 MPa. The pressed samples were sintered in an electrical furnace (Carbolite, 1700) without the application of pressure at 1500 °C for 1 h in an inert atmosphere. The speeds of heating and cooling remained constant and were 10 $Kminute^{-1}$. The characterization of sintered products was carried out in the following way; the density was evaluated by the Archimedes' method, the hardness was measured with the help of Vickers indenter, the fracture toughness was determined by the method of fracture by indentation using the equation of Evans. Reported values are the average of ten measurements. The microstructures of the composites were observed with the help of a scanning electron microscope (SEM). The SEM was equipped with energy dispersive X-ray spectrometer (EDX) with which the phases present in the microstructure could be identified.

### 3.3 Results and discussion

#### 3.3.1 Microstructure

Figure 9. Shows typical microstructures obtained by SEM of some of the composites investigated. Here, it can be seen fine and homogeneous microstructures, with the presence of two phases, on the basis of (EDX) analysis, it is deduced that the gray phase corresponds to the alumina matrix and the small white and brighter phase corresponds to the metallic reinforcement added to the ceramic matrix. The metallic phase is localized principally at intergranular positions. The main metallic particle size is on average 1 μm. In general all microstructures are fine, however the use of Ni, Ti and the corresponding intermetrallics help to obtain the finest microstructures in the composites. Judging from the trend disclosed by the $Al_2O_3$/intermetallic composites, it can be noticed that the microstructures have no cracks or pores, thus suggesting that the in situ formation of the intermetallics did not just occur, but in addition helped in the diffusion process in order to obtain well consolidated bodies. Image analysis performed on all the samples studied showed that the average volume fraction of the metallic phase in the composites was approximately 9.5%.

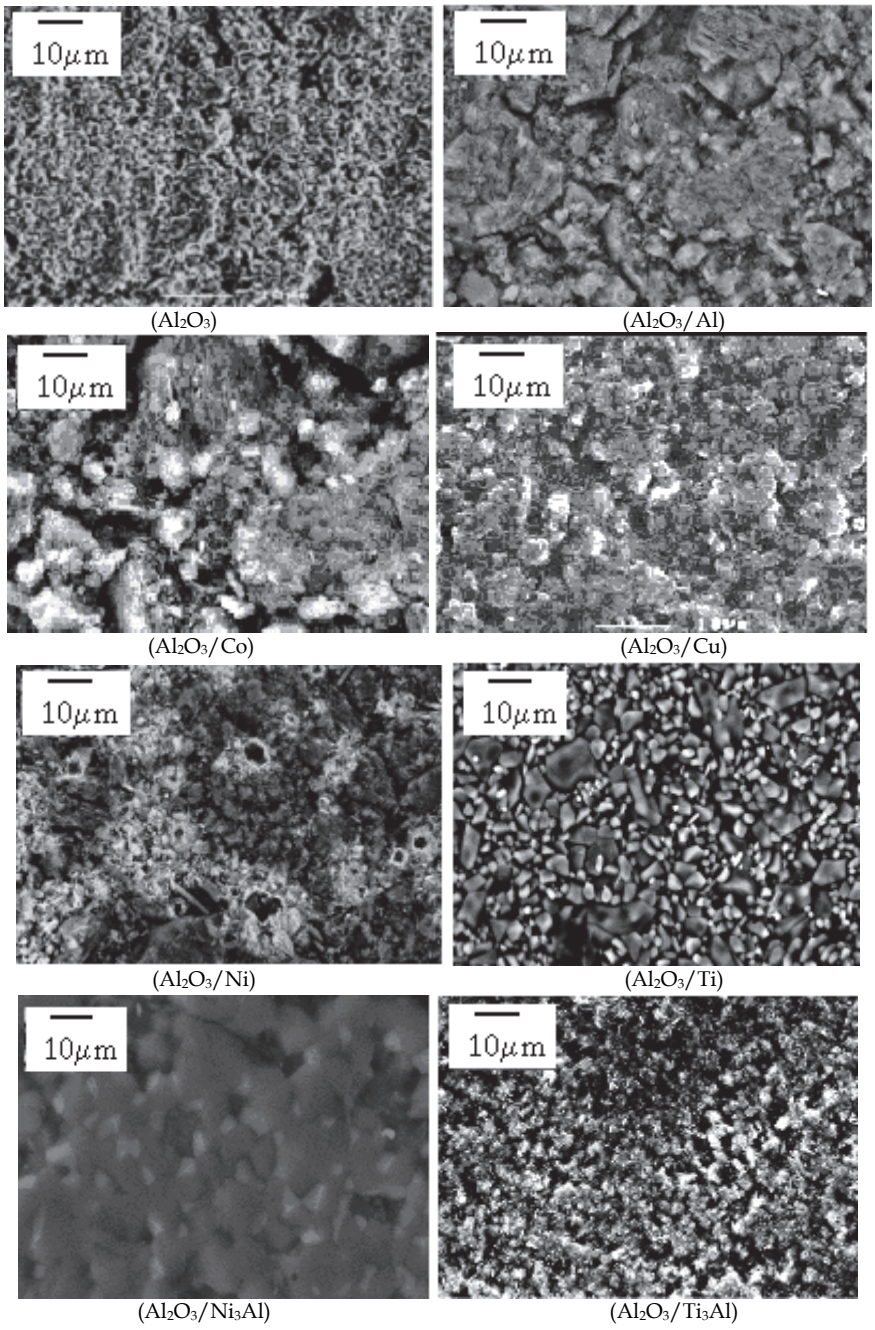


Fig. 9. Typical microstructures obtained by scanning electron microscopy of some of the composites investigated here.

The values of density, hardness and fracture toughness evaluated in the composite materials fabricated here are reported in Table 1. In this table also are reported the corresponding values for monolithic $Al_2O_3$ also processed here.

| Reinforced Metal | ρ relative (%) | HV (GPa) | $K_{IC}$ (MPa·m$^{-1/2}$) |
|---|---|---|---|
| **$Al_2O_3$** | 94.95 +/- 1.2 | 20.97 +/- 1.7 | 3.2 +/- 0.2 |
| **Al** | 89.01 +/- 0.88 | 18.62 +/- 1.3 | 4.1 +/- 0.1 |
| **Co** | 96.64 +/- 0.79 | 18.61 +/- 1.4 | 4.3 +/- 0.1 |
| **Cu** | 93.32 +/- 0.91 | 18.90 +/- 1.2 | 4.4 +/- 0.1 |
| **Fe** | 92.82 +/- 1.10 | 18.51 +/- 1.5 | 4.0 +/- 0.1 |
| **Mo** | 89.17 +/- 0.93 | 19.03 +/- 1.3 | 4.1 +/- 0.1 |
| **Ni** | 96.35 +/- 0.80 | 18.11 +/- 1.4 | 4.7 +/- 0.1 |
| **Ti** | 98.25 +/- 0.83 | 18.17 +/- 1.5 | 4.8 +/- 0.1 |
| **Zr** | 92.59 +/- 0.88 | 19.10 +/- 1.6 | 4.2 +/- 0.1 |
| **$Fe_3Al$** | 95.40 +/- 0.94 | 18.78 +/- 1.2 | 5.2 +/- 0.2 |
| **$Ni_3Al$** | 98.30 +/- 0.97 | 16.43 +/- 1.4 | 6.9 +/- 0.2 |
| **$Ti_3Al$** | 98.52 +/- 1.10 | 16.10 +/- 1.6 | 7.3 +/- 0.2 |
| **$Zr_3Al$** | 98.76 +/- 0.89 | 18.12 +/- 1.5 | 7.0 +/- 0.2 |

Table 1. Values of relative density, hardness and fracture toughness of the different $Al_2O_3$-based composites fabricated here.

### 3.3.2 Density

From this table it can be observed that the composite materials reinforced with Al, Cu, Fe, Mo and Zr display a lower relative density than monolithic $Al_2O_3$, whereas the composite materials reinforced with the other metals (Co, Ni and Ti) including all the intermetallics used, show better densification than monolithic $Al_2O_3$. The worst densifications were obtained in composites with Al and Mo, this may be due to the big differences in densities and melting points between these two metals in comparison with the corresponding values of monolithic $Al_2O_3$. This difference provokes poor diffusion during the sintering stage, leading to heterogeneous microstructures and in consequence bad densification of the products. For the cases were good densifications were obtained, as well as for the cases where in situ intermetallics were formed, in addition the reactions allowed some diffusion mechanisms to be activated during the process helping the densification of the products. The densification of the reinforced sample with titanium was very good, and it was equivalent to the densification obtained with the intermetallics. This was due probably to the close relation between the densities of titanium, the intermetallics and $Al_2O_3$, a situation than helps atomic movement during the sintering.

### 3.3.3 Hardness

With respect to the hardness results, from table 1 it can be seen that for all the systems monolithic $Al_2O_3$ is the hardest material. All the composite materials present hardness values between 18 and 19 GPa that are less than the almost 21 GPa reported for monolithic $Al_2O_3$. This is logical because a ceramic material has to be harder than the same ceramic material with the incorporation of ductile phases in its bulk volume.

### 3.3.4 Fracture toughness

From Table 1 and Figure 10 it can be observed that in all the composite cases the fracture toughness of monolithic $Al_2O_3$ was improved considerably, principally in composites reinforced with Ni and Ti and in all composites reinforced with intermetallic phases. The incorporation of ductile metal particles in the ceramic matrix enhances the fracture toughness due to plastic deformation of the metallic phase, which forms crack-bridging ligaments when a crack grows in the material under a tensile stress action. In other words, the energy absorbed for plastic deformation is unavailable for crack extension. Additionally, the deformed particles could bridge the faces of the crack wake, thereby exerting closure stresses, reducing the effect of the stress intensity at the crack tip (Ji & Yeomans, 2002; Lalande, 2003).

For the case of $Al_2O_3$/Ni system: nickel provides a liquid phase during the sintering stage that promotes diffusion and therefore densification of the composite On the other hand, Ni helps to refine the alumina microstructure by pinning its grain boundaries and thereby restraining the grain growth of alumina.

For the case of the $Al_2O_3$/Ti system: because the densities of titanium and alumina are very similar, Ti is well dispersed in the alumina matrix, forming a good homogeneous composite microstructure that promotes diffusion and densification, and as a consequence good toughening of the final material.

For the case of $Al_2O_3$/intermetallics systems: the use of intermetallics as reinforcement in $Al_2O_3$ gives an appreciable enhancement in the fracture toughness, this is due to the good ductility, low density and chemical compatibility of intermetallics with alumina. These factors help to obtain homogeneous microstructures with the formation of interfaces that allow the activation of different diffusion mechanisms thus improving the final density and then the mechanisms that improve the fracture toughness of the composites.

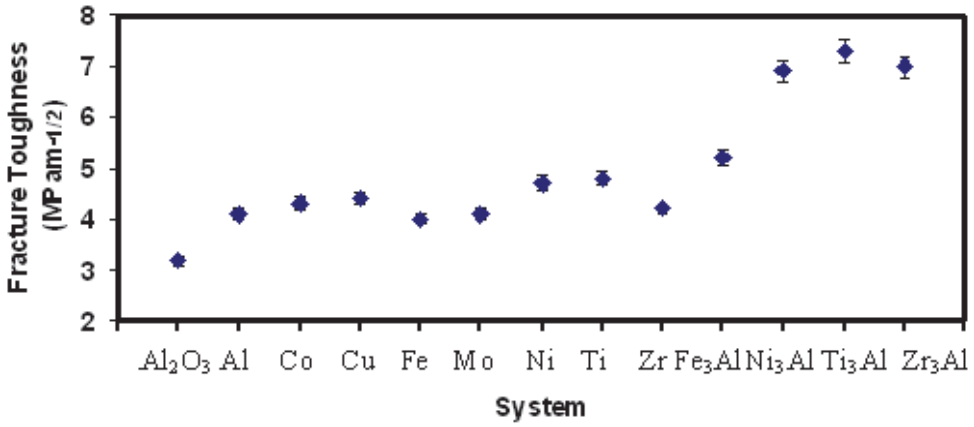


Fig. 10. Fracture toughness values measured for all the composites investigated.

Figures 11a and 11b show the fracture surface and the advance of a crack in an $Al_2O_3$/Ti reinforced composite. The fracture mode in figure 11a corresponds to microvoid coalescence as suggested by the dimple-like depressions that are typical of ceramic materials. From figure 11b it can be observed that the sample exhibits a mixed fracture mode, because metallic particles bridge the surface of the crack in the composite, but at the same time they

can cause deflection of the crack. So the toughening mechanism in $Al_2O_3$/metal reinforced composites is due to crack bridging and crack deflection in this type of material. Steinbrech has reported that the improvement achievable in reinforced composites is governed by the mechanical properties of the ductile material, ligament diameter, volume fraction of the components, interfacial properties and the reaction products of the constituents (Steinbrech, 1992). This can explain the differences obtained in the fracture toughness of the materials investigated here.

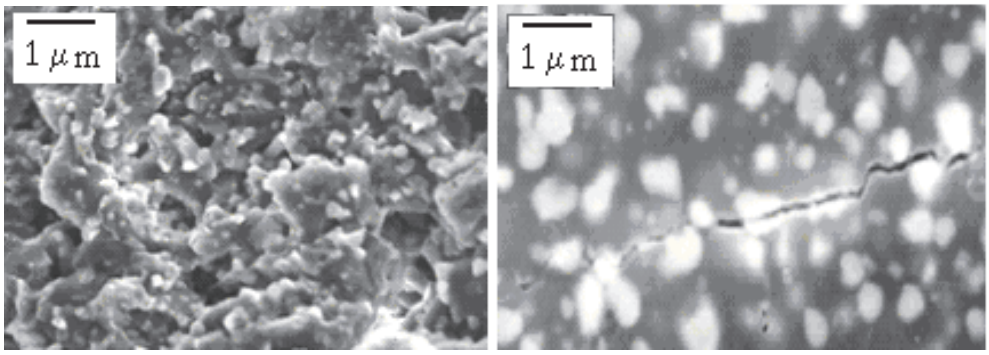


(a) (b)

Fig. 11. (a) Fracture surface and (b) advanced of a crack in an $Al_2O_3$/Ti reinforced composite.

## 4. Conclusions

$Al_2O_3$-based composites reinforced with different metals have been fabricated by both; liquid and solid pressureless sintering of an intensive mechanical mixture of powders. By the use of ductile particles in a hard ceramic matrix, significant improvements in fracture toughness due to plastic deformation of the metallic phase has been obtained. However, there are metals that enhance the toughness of a ceramic better than others; these are those metals that have similar densities to alumina, because they help to obtain fine and homogeneous microstructures after sintering. From the fracture toughness measurements and microstructural observations, finally it can be commented that the toughening mechanism in $Al_2O_3$/metal reinforced composites is due to crack bridging and crack deflection.

Through fabricated composite-materials it was possible to analysis the application of the indentation fracture (IF) method for the determination in a simple and reliable way the fracture toughness of those materials. From the obtained results and with the help of bases given in the literature it can be commented that the main requirements to be met for samples that will be applied the IF methods for their fracture toughness determination are:

- Porosity fine and well distributed.
- Homogeneous microstructure.
- Good surface finish, free of residual stresses, pores and cracks.
- Parallel surfaces

## 5. Acknowledgements

Author would thank to the mixed foundation of promotion to the scientific and technological investigation from CONACyT-Tamaulipas Government, by the support offered for the accomplishment of the research work and its diffusion.

## 6. References

Anstis G. R., Chantikul P., Lawn B. R., and Marshall D. B. (1981). A Critical Evaluation of Indentation Techniques for Measuring Fracture Toughness: I, Direct Crack Measurements, *Journal of the American Ceramic Society*, Vol. 64, No. 9, (September 1981) pp. 533–538.

ASTM E1820 - 09e1 Standard Test Method for Measurement of Fracture Toughness. (2008) *Annual Book of ASTM Standards*, (2008).

ASTM C 1327-99, Standard Test Method for Fractute Toughness at Room Temperature of Advanced Ceramics (1999). *Annual Book of ASTM Standards*, (1999), pp. 14-02.

Bhat S. (2006). Fracture parameters estimation of alloy steel reinforced with maragin steel. *Fracture of Nano and engineering Materials and Structures, Proceedings of the 16th European Conference of Fracture*, Alexandroupolis Grecce, Edited by Gdoutos E. G. (July, 2006), pp.

Boch P., Chartier T. and Giry J. P. (1990). Zirconio Toughened Mullite / The Role of Circón Dissociation, *Ceram. Trans., Mullite and Mullite Matrix Composites*, edited by Somiya S., Davies R. F. and Pak J.A. Vol. 6, (1990), pp. 473-494.

Evans A. G. and Charles E. A. (1976). Fracture Toughness Determination by Indentation, *J. Am. Ceram. Soc.*, Vol. 59, (1976), pp. 371-372.

Griffith A. A. (1921). The Phenomena of Rupture and Flow in Solids, *Phil. Trans*. R. Soc. Lond. (January, 1921) pp. 163-198.

Ji Y. and Yeomans J. (2002). Processing and mechanical properties of $Al_2O_3$-5 vol.% Cr nanocompistes. *J. Eur. Ceram. Soc*., Vol. 22, No. 12 (2002) pp. 1927-1930.

Konopka K. and Szafran M. (2006). Fabrication of $Al_2O_3$-Al composites by infiltration method and their characteristics. *J. Mater. Proc. Technol*., Vol. 175, (2006), pp. 266-270.

Lalande J., Scheppokat S., Jansen R. and Claussen N. (2002). Toughening of alumina/zirconia ceramic composites with silver particles. *J. Eur. Ceram. Soc*., Vol. 22, No. 13 (2002) pp. 2165-2168.

Lieberthal M. I. and Kaplan K. (2001). Processing and properties of $Al_2O_3$nanocomposites reinforced with sub-micron Ni and $NiAl_2O_4$. *Mater. Sci. Eng*., Vol. A302, No. 1 (2001), pp. 83-91.

Marci C. and Katarzyna P. (2007). Processing, microstructure and mechanical properties of $Al_2O_3$-Cr nanocomposite *J. Eur. Ceram. Soc.*, Vol. 27. No. 2-3, (2007), pp. 1273-1277.

Marshall D. B. and Lawn B. R. (1986). Indentation of Brittle Materials", *Microindentation Techniques in Materials Science and Engineering, ASTM* Vol. 889, (1986), pp. 26-46.

Miranda Hernández J. G., Moreno Guerrero S., Soto Guzmán A. B. and Rocha Rangel E. (2006). Production and Characterization of $Al_2O_3$-Cu Composite Materials. *J. Ceram. Proc. Res*., Vol. 7, No. 4, (2006), pp. 311-315.

Niihara K., Morena R. and Hasselman D. P. H. (1982). Evaluation of $K_{IC}$ of Brittle Solids by The Indentation Method with Low Crack-To-Indentation Ratios, *J. Mater. Sci. Lett.*, Vol. 1, (1982), 1, pp. 13-16.

Plaza L. M. (2003). Determination of Uncertaines in Plane Tougness ($K_{IC}$) Testing, *Seminario Sobre la Evaluación de la Incertidumbre en Ensayos Mecánicos*, Universidad de la Rioja, España, (2003).

Steinbrech R. W. (1992). Toughening mechanisms for ceramics materials. *J. Eur. Ceram. Soc.* Vol. 10, No. 3 (1992) pp. 131-135.

Sglavo V. M., Marinob F., Zhang B. R. and Gialanella S. (1997). $Ni_3Al$ intermetallic compound as second phase in $Al_2O_3$ ceramic composites. *Mater. Sci. Eng.*, Vol. A239-240, (1997), pp. 665-669.

Travirskya N., Gotmanb I. and Claussen N. (2003). Alumina-Ti aluminide interpenetrating composites: microstructure and mechanical properties. *Mater. Lett.*, Vol. 57, No. 22-23, (2003), pp. 3422-3424.

Wang C. H. (1996). Introduction to Fracture Mechanics, *DSTO Aeronautical and Maritime Research Laboratory*, (July, 1996), pp. 199-207.

Weisbrod G. and Rittel D. A. (2000). Method for Dynamic Fracture Toughness Determination Using Short Beams, *International Journal of Fracture*, Vol. 104, (2000), pp. 1-5.

Wessel J. K. (2004). *The Handbook of Advanced Materials*. John Wiley & Sons, USA (2004).

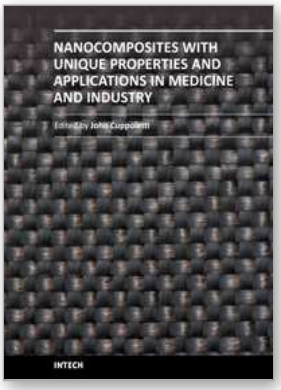


**Nanocomposites with Unique Properties and Applications in Medicine and Industry**

Edited by Dr. John Cuppoletti

ISBN 978-953-307-351-4
Hard cover, 360 pages
**Publisher** InTech
**Published online** 23, August, 2011
**Published in print edition** August, 2011

This book contains chapters on nanocomposites for engineering hard materials for high performance aircraft, rocket and automobile use, using laser pulses to form metal coatings on glass and quartz, and also tungsten carbide-cobalt nanoparticles using high voltage discharges. A major section of this book is largely devoted to chapters outlining and applying analytic methods needed for studies of nanocomposites. As such, this book will serve as good resource for such analytic methods.



INTECH
open science | open minds

**InTech Europe**
University Campus STeP Ri
Slavka Krautzeka 83/A
51000 Rijeka, Croatia
Phone: +385 (51) 770 447
Fax: +385 (51) 686 166
www.intechopen.com

**InTech China**
Unit 405, Office Block, Hotel Equatorial Shanghai
No.65, Yan An Road (West), Shanghai, 200040, China
中国上海市延安西路65号上海国际贵都大饭店办公楼405单元
Phone: +86-21-62489820
Fax: +86-21-62489821